CHEMISTRY OF MATERIALS



Article

# FUNCTIONAL NETWORKS OF ORGANIC AND COORDINATION POLYMERS: CATALYSIS OF FRUCTOSE CONVERSION

Lev Bromberg, Xiao Su, and T. Alan Hatton

*Chem. Mater.*, **Just Accepted Manuscript** • DOI: 10.1021/cm503098p • Publication Date (Web): 23 Oct 2014

# FUNCTIONAL NETWORKS OF ORGANIC AND COORDINATION POLYMERS: CATALYSIS OF FRUCTOSE CONVERSION

Lev Bromberg, Xiao Su, T. Alan Hatton*

Department of Chemical Engineering, Massachusetts Institute of Technology,

Cambridge, MA 02139. *E-mail tahatton@mit.edu

## Abstract

The creation of functional porous nanoscale networks with enhanced reactive group accessibility provides rich promise for novel designs of composite materials. We present a straightforward strategy for the preparation of porous polymer/MOF hybrids via polymerization of organic monomers and crosslinkers impregnated within the pores of the MOFs followed by functionalization of the resulting composite. A poly(maleimide-*co*-dibinylbenzene) network was synthesized in the presence of MOF MIL-101(Cr), resulting in stable hybrid composites, which were then brominated to give porous hybrids of crosslinked poly(N-bromomaleimide), a polymeric analogue of N-bromosuccinimide, interconnected with crystalline nanoparticles of the MOF. Due to the large porosity and surface area, the active bromine (halamine) groups in the polymer network enabled high activity of the composites in heterogeneous catalysis of conversion of D-fructose into 5-hydroxymethylfurfural.

## Introduction

The environmental and energy challenges facing the global community today require creative and innovative solutions that will most likely be based on new structured materials with enhanced, tailored properties. For instance, diverse chemistries, high surface area and porosity

of metal-organic frameworks (MOFs) built into 3D crystalline structures from alternately connecting metal ions and organic linkers make these materials exceptionally promising in applications ranging from gas storage and catalysis to proton conduction and lithium batteries.[1-7] Due to the highly ordered porous structures, MOFs can be used as sacrificial templates and/or precursors to yield, via carbonization processes, porous carbon materials with nanostructured metal/metal oxide components.[6,8] In addition to MOFs, porous organic polymers (POPs), a class of amorphous polymers exhibiting permanent microporosity, appear to be resourceful materials for potential applications in gas storage, separation, and catalysis.[9-11] POPs are constructed from rigid monomers that can cross-link into networks with pores of uniform size. The chemical stability of microporous organic networks makes them ideal for supporting chemical reactions without framework destruction or loss of porosity. Polymerization in confined spaces of POPs or MOFs affords hybrid nanocomposites with previously unknown architectures and functionalities.[12-16] By radical polymerization of monomers such as styrene, methylmethacrylate, vinyl acetate, etc. in microporous regular channels of MOFs, Kitagawa and co-authors managed to control dimensionality and stereoregularity of the resulting polymers.[15,16] The MOF structures were used as sacrificial templates in the polymerizations resulting in polymers of well-defined architecture, shape and size, which had been difficult to attain by conventional polymer synthesis means. Similarly, a recent report described polymerization of vinylbenzyl trimethylammonium hydroxide in MOF in zeolitic imidazolate framework (ZIF-8) resulting in a composite capable of ion-exchange.[17]

Herein, we describe a straightforward strategy for the synthesis of novel, functional composite materials that are hybrids of MOFs and polymer networks. These hybrids demonstrate potential for the facile synthesis of high-value chemical intermediates from renewable resources,

specifically by the dehydration of fructose. In our strategy (Fig.1), the MOF porous structure is impregnated with organic monomers and crosslinkers, which are then polymerized in-situ (P) and functionalized (F) to form the resulting hybrid nanocomposite. Although the polymer network fills some of the MOF pores, the surface area of the hybrid is still large, and the open structure of the MOF enables ready access of the reactants to the functional groups on the polymer chains situated on the pore surfaces. Chemical and structural stability of the hybrid composite is enabled by the intertwined, interlocked structure wherein the polymer chains threading through the pores of the MOF are locked in place by covalent cross-linking. We chose MIL-101(Cr) as the MOF component for a hybrid because of its excellent stability and open pore structure with large, ~3.6 nm cavities accessible through 1.2-1.5 nm windows. [18] Large cavities of MIL-101(Cr) can be accessed by molecules of 13–14 Å in diameter through the impregnation-diffusion approach.[18,19] Maleimide was our monomer choice for the hybrid due to its small molecular size (MW 97 g/mol), ease of free-radical (co)polymerization via a very reactive double bond, and presence of the -C(O)NHC(O)- functional imide group that is susceptible to halogenation and other reactions. We have shown previously that non-porous poly(N-bromomaleimide-*co*-divinylbenzene) networks are active solid-phase oxidants in reactions with phosphorothioates, thioethers, and hydrazines due to the polymer's active >N-Br groups.[20] In this work, we found the MOF-brominated polymer hybrids to be potent heterogeneous catalysts for the industrially important reaction of fructose conversion to 5-hydroxymethylfurfural (HMF). We envision that the simple and effective method of fabrication of hybrid, functional porous

networks will promote the development of materials for a wide spectrum of applications.

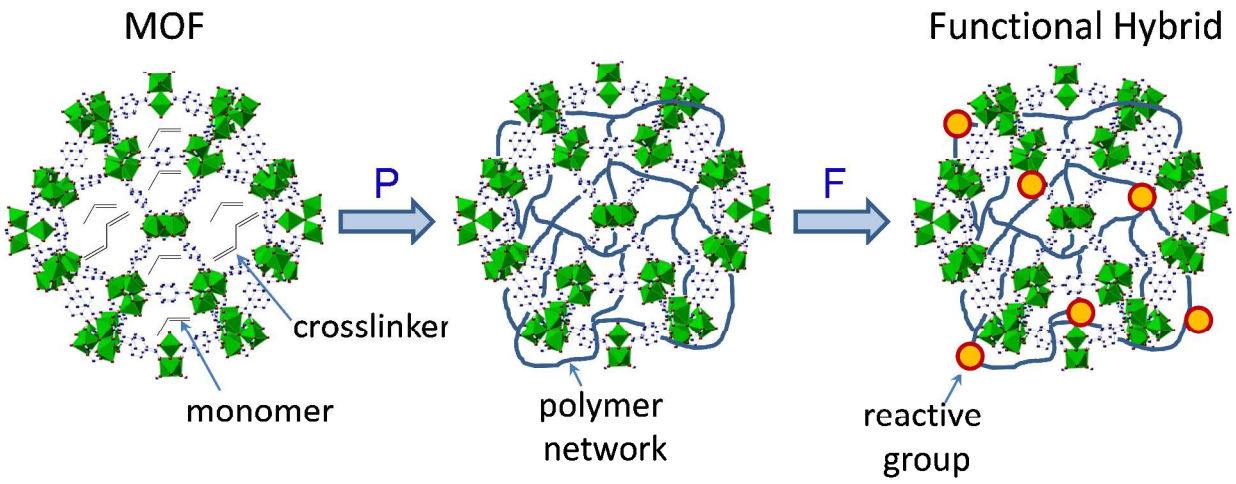


**Fig.1**. Scheme of fabrication of functional hybrids of MOFs and polymer networks. MOF impregnated by monomer and crosslinker is subjected to in-situ polymerization (P) followed by functionalization (F) by a reactive group.

## Experimental

### Materials

All chemicals and solvents used were obtained from Sigma-Aldrich Chemical Co. and were of the highest purity available.

### Syntheses

#### Polymaleimide-based crosslinked networks (PMAi-*co*-DVB) [20]

PMAi-*co*-DVB networks were synthesized by free-radical copolymerization of maleimide and divinylbenzene. In a typical synthesis, a solution of maleimide (970 mg, 10 mmol), divinylbenzene (390 mg, 3 mmol) and dicumyl peroxide (100 mg, 0.37 mmol) in 10 mL dioxane was deoxygenated by freeze-thaw and nitrogen bubbling for 0.5 h and then kept at 80$^{o}$C in a sealed flask for 24 h. The resulting white solid was twice dispersed in excess diethyl ether,

separated and then dispersed sequentially in acetone and methanol and then separated by filter-suction and dried under vacuum until constant mass. The yield of polymerization was measured to be approximately 90 wt% relative to the initial maleimide loading. The effect of DVB concentration on the solubility of the resulting networks by 24 h extraction in methanol and acetonitrile was studied. At an initial DVB/maleimide concentration ratio below 0.15 mol/mol, a 10-20 wt% fraction of the network appeared to be soluble, and thus the DVB/maleimide mol/mol ratio of 0.15 to 0.3 was deemed to be suitable for the further network studies.

**MOF MIL-101(Cr)**

Particles of MOF MIL-101(Cr) were synthesized hydrothermally without the use of hydrofluoric acid, utilizing an autoclave oven heat supply (S-1).[19]

**Hybrid MOF- PMAi-*co*-DVB composites**

In a typical synthetic procedure, dry, powdered MOF MIL-101(Cr) was placed in a solution containing 970 mg (10 mmol) maleimide, 284 μL (2 mmol) divinylbenzene, 82 mg (0.3 mmol) dicumyl peroxide and 10 mL dioxane. The mixture was sonicated for 30 s to disperse the MOF particles, deaerated by freeze-thaw and nitrogen purge for 0.5 h, sealed and kept at 80$^{o}$C for 24 h. The resulting solids were crushed and washed sequentially with excess methanol, acetone, and water. The particles were dried at 80$^{o}$C for 8 h and then lyophilized under high vacuum to dryness for 2 days. Separate synthetic procedures with varying initial MOF/maleimide ratios were also conducted. Dry, ground composite materials with the initial divinylbenzene/imidazole ratio of 0.2 mol/mol were subjected to *stability studies*. There was no visible separation of flaky smaller particles after grinding. Likewise, when the polymerized material was suspended in deionized water at 90$^{o}$C or DMSO at 100$^{o}$C overnight with occasional shaking, some solvent uptake by the composite was observed, but the MOF particles could not be mechanically

separated from the larger composite particles using flotation and centrifugation (5000 g, 15 min). The chemical stability was accessed by elemental analysis of the wash-outs in methanol after 8-h Soxhlet extraction of 10 mg/mL composite suspension at 70$^{o}$C. Under harsh conditions, only ca. 0.05 wt% of Cr and 0.9 wt% of carbon initially present in the composite particles were lost. After equilibration of 10 mg/mL composite suspension in deionized water at 90$^{o}$C for 3 h and particle separation by centrifugation at 12,000 g, elemental analysis of the wash-outs demonstrated below 1 wt% of the initial chromium and carbon were leached into water. The MOF component of the composite was totally dissolved in 1 M aqueous NaOH at 90$^{o}$C within 3 h. Polymerized in the presence of MOF without any crosslinker, poly(N-maleimide) (PMAi) could be extracted readily from the composite by equilibration in DMF at 70$^{o}$C for 8 h. Weight-average molecular weight of the extracted polymer was measured to be 60 kDa (polydispersity, 2.4). Exposure of the composite particles to DMSO at 100$^{o}$C followed by particle removal by centrifugation at 12,000 g and elemental analysis of the residual solvent for Cr yielded insignificant chromium concentration (<10-20 ppb, or less than 0.1% of the initially present Cr), demonstrating stability of the composites.

**Composite functionalization**

Finely powdered, dry PMAi-*co*-DVB or MOF-PMAi-co-DVB network (1 g) was suspended in a glass flask with chilled, freshly prepared 20 wt% bromine solution in carbon tetrachloride (15 mL) at 0$^{o}$C under constant stirring. The suspension was sealed and brought up to ambient temperature within 4 h under stirring, which continued for another 20 h. The suspension was extraction-washed by carbon tetrachloride, deionized water, and acetone and the solids were carefully separated by suction filtration. The solids were again washed by acetone and dried under vacuum. Bromine contents of the resulting brominated polymer network

(abbreviated PMAi-Br) and composite material (henceforth abbreviated MOF-PMAi-Br) were measured by titration as described previously [20] to be 3.9 and 1.8 meq/g, respectively. The yield of the bromination reactions was at least 92 wt% relative to the initial polymer in the composite material. For PMAi-Br, calc.: C, 33.5; H, 1.92; Br, 41.0; N, 7.19; found: C, 34.4; H, 1.66; Br, 41.9; N, 7.34. For MOF-PMAi-Br, calc.: C, 46.0; H, 2.65; Br, 13.8; Cr, 6.22; N, 2.61; found: C, 46.3; H, 2.56; Br, 14.1; N, 2.48.

**Monosaccharide conversion and HMF yield measurements**

The progress of the fructose dehydration in DMSO with time was followed by NMR measurements (S2). [21,22]

Conversion of fructose and glucose into 5-hydroxymethylfurfural (HMF) in DMSO was quantified using a PerkinElmer Flexar™ FX-15 ultrahigh performance liquid chromatograph, according to established protocols. [23-26] The HPLC system included PekinElmer UV/Vis and refractive index (RI) detectors for measurement of HMF and fructose, respectively, and PerkinElmer Brownlee Analytical columns: DB C18 (150 mm x 4.6 mm x 5 μm) and Amino (150 mm x 4.6 mm x 3 μm, 110 Å). In experiments with glucose, only HMF yield was measured at 2 and 6 h after the reaction commencement. The columns were maintained at 35°C, the mobile phase was deionized water adjusted to pH 4.0 by HCl, with a flow rate of 0.7 mL/min and an injection volume of 2 μL. An assay was developed where calibration curves (absorbance at λ= 284 nm *vs* concentration for HMF, and refractive index units *vs* concentration for fructose) and the retention times for HMF and fructose were determined using solutions of pure compounds in the same mobile phase. The reaction experiments were performed at 100°C in stoppered glass tubes immersed in a thermostatted oil bath and stirred using magnetic stirring bars. Prior to equilibration at elevated temperatures, D-fructose solutions in DMSO (concentrations, $C_{f0}$,

ranging from 0.055 to 0.55 M) were deaerated by nitrogen flow and were stored frozen at 4°C to prevent any premature reactions from occurring. Prior to the commencement of the reaction measurements, the solutions (5 mL) were deaerated by nitrogen and briefly (10-30 s) sonicated at ambient temperature with the added catalysts for the catalyst dispersal and immersed in the heating bath while stirring vigorously. Samples (15-75 μL) were withdrawn at predetermined time intervals and immediately diluted 10-fold by water (pH 4.0). After brief sonication, the diluted samples were centrifuged for 30 s at 12,000 *g* to remove residual catalyst particles and insoluble reaction products, if any, and the resulting clear solutions were subjected to the HPLC analysis. The reaction progress was characterized by fructose fractional conversion (*F*) and HMF yield (*Y*):

$$F = 1 - C_f / C_{f0} \quad (1)$$

$$Y = 100 \cdot \left( C_{\mathrm{HMF}} / C_{f0} \right) \text{ mol\%} \quad (2)$$

where $C_{f0}$ and $C_f$, are the concentrations of fructose in the sample initially and at time *t*, respectively, and $C_{\mathrm{HMF}}$ is the concentration of HMF in the sample at time *t*. Based on eqns (1) and (2), the selectivity of the fructose conversion to HMF, *S*, can be defined as $S = (Y/F)$.

*"Hot filtration" experiments* [27-30] were conducted to evaluate the effects of the MOF-PMAi-Br removal from the reaction medium on the rate of D-fructose conversion and HMF yield (S-3).

*Catalyst recycling* was accomplished by retrieval of the solid MOF-PMAi-Br catalyst after 1 h of the fructose reaction by centrifugation of the entire reaction medium at 12000 g for 1 min, solids separation and repeated washing by deionized water, ethanol and acetone. The washed catalyst was dried under vacuum and placed in a fresh fructose solution in DMSO at 100°C. Multiple fractions of the catalyst that underwent 4 cycles were combined and subjected to powder XRD measurement to evaluate the effect of the catalyst reuse on its crystal structure. The

catalyst that underwent 4 cycles was collected and subjected to regeneration via bromination with bromine in $CCl_4$ as described above.

**General Methods**

Scanning electron microscopy (SEM) images were taken with a Zeiss Merlin high-resolution SEM and FEI/Philips XL30 FEG ESEM microscope at 20 kV accelerating voltage, a 1000-4000x magnification, and a working distance of 10.1 mm using low vacuum with $H_2O$ pressure of 0.5 Torr. The samples were mounted on a conductive copper tape. TEM was performed on a JEOL 200-CX transmission electron microscope. Energy dispersive X-ray spectroscopy (EDS) data were obtained using an EDAX probe with a resolution of 512 x 400 at 1200x magnification, 99 frames and 50 μm dwell time. Surface area measurements were conducted using an Accelerated Surface Area and Porosimetry Analyzer ASAP 2020 (Micromeritics Corp.) at liquid nitrogen temperature (77 K). Prior to each adsorption measurement, the sample was degassed at 323 K under vacuum for 16 h. The specific surface areas were evaluated using the Brunauer-Emmett-Teller (BET) method in the $P/P_0$ range of 0.06-0.20. Pore size distribution curves were calculated using the Barrett-Joyner-Halenda (BJH) method from the desorption branch of the isotherms and pore sizes were obtained from the peak positions of the distribution curves. Thermogravimetric analysis (TGA) was conducted using a Q600 thermogravimetric analyzer (TA Instruments, Inc.). Samples were subjected to heating scans (20 °C/min) under a nitrogen atmosphere and in a temperature ramp mode. FTIR spectroscopy was performed with a Nicolet 8700 FTIR spectrometer (Thermo Scientific Inc.) using KBr pellets. Spectra were recorded over the wavenumber range between 4000 and 400 $cm^{-1}$ at a resolution of 1 $cm^{-1}$ and are reported as the average of 64 spectral scans. $^1H$ and $^{13}C$ NMR spectra were collected at 25 ± 0.5 °C using a Bruker Avance-400 spectrometer operating at

400.01 and 100 MHz, respectively. X-ray powder diffraction (XRD) patterns were acquired for 24 h with a Panalytical X'Pert Pro multipurpose diffractometer equipped with an X'celerator high-speed detector coupled with a Ni β-filter and using the Cu Kα radiation at room temperature. Samples were packed in a ZBH placeholder. Programmable divergence slits were used to illuminate a constant length of the samples (4 mm). The published XRD pattern for MIL-101 was used as the reference pattern. Peak assignment and structure refinement were accomplished with X'Pert Highscore Plus v3 software. XPS measurements were performed using a PHI Versaprobe II Scanning XPS Microprobe (ULVAC, PHI). The survey scans were performed with a 200 μm area scan with 50 W power and 15 kV, with a pass energy of 180 eV with ion gun neutralization. The survey was performed from 0 to 1100 eV, with 10 cycles and 0.1 eV accuracy. The depth of measurement is between 4 to 10 nm. The high resolution scans were performed on C1s, O1s, N1s, Cr2p and Br3d with 2 cycles and 10 scans each at 0.05 eV steps and 11.5-24 eV pass energy.

**Results and Discussion**

The monomer and crosslinker were polymerized in MOF particle suspensions in dioxane, and then dried to form a white solid powder. This solid product was washed, dried again, and crushed to give 100-300 μm particulates that contained ~20-50 nm octahedral MOF particles distributed throughout the polymerized material (Fig.2 and S4).

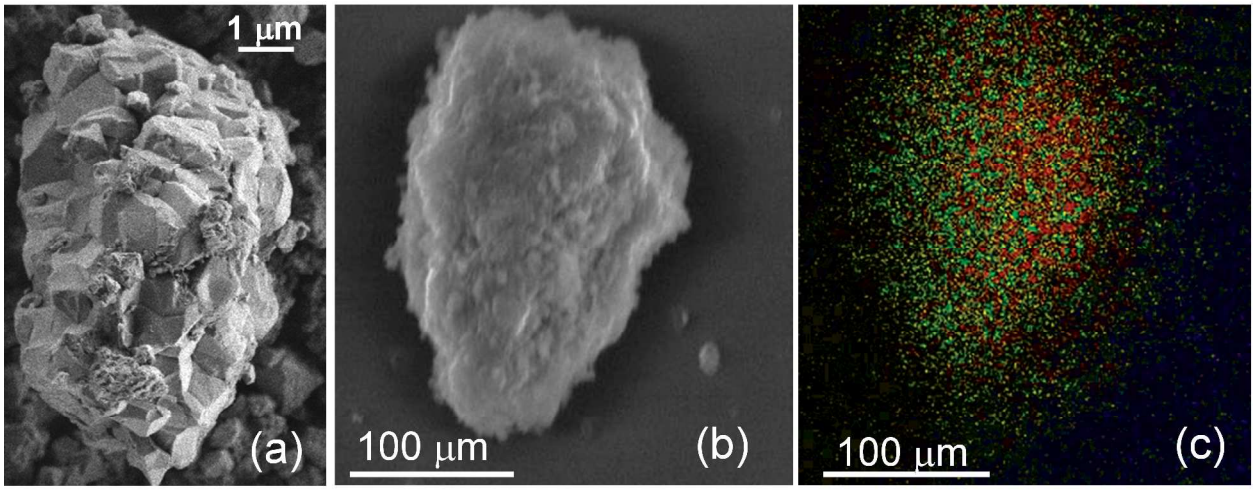


**Fig.2**. High-resolution SEM image of a MOF-PMAi-Br composite particle on the Zeiss Merlin SEM under high vacuum and 5 kV (a) and EDS mapping analysis of the composite shown on the same scale on the Philips XL 30 FEI SEM at 15 kV (b,c). In c, green and red dots show chromium and bromine, respectively.

High chemical and compositional stability of composites with an initial divinylbenzene/maleimide ratio of 0.2 mol/mol was observed in water and organic solvents (see Experimental). The absence of a polymer/MOF phase separation or of leaching of the components by water and organic solvents supports the notion of stable interlocked composite structures (Fig.1). EDS chemical composition mapping demonstrated that both Cr and Br elements were evenly distributed across the brominated composite particles, MOF-PMAi-Br (Fig.2, b,c).

Hybrid, bromine-functionalized composites and their parent MOF and non-functionalized MOF-PMAi materials and corresponding PMAi-Br polymer networks were characterized by nitrogen

sorption isotherms (Fig.S5), thermogravimetric analysis (Fig.S6), FTIR (Fig.S7), XPS (Fig.S8) and powder XRD spectroscopy (Fig.S9).

The PMAi and PMAi-Br polymer networks did not show any appreciable porosity, with BET surface areas measured to be in the range of 10-20 $m^2/g$. In contrast, the MOF-PMAi-Br composites appeared to be porous, with BET and Langmuir surface areas in the ranges of 1100-1600 and 1600-1800 $m^2/g$, respectively. The BJH desorption pore diameter was in the 2.0-2.9 nm range. The surface areas of the MOFs depended strongly on their post-synthesis treatment. The *as-prepared* MOF possessed BET and Langmuir surface areas of 1350 and 1690 $m^2/g$, respectively, whereas the MOF activation brought these parameters up to 3500 and 4300 $m^2/g$, respectively. The surface area of the composites of MOF that underwent impregnation, polymerization and bromination was also affected by whether or not the parent MOF was activated prior to its impregnation. The $MOF_a$-PMAi-Br composite resulting from the activated MOF possessed a BET area that was ca. 10-15% higher than that of its counterpart based on the non-activated MOF.

Bromine titration, FTIR, XPS and elemental analysis all indicated that the mass ratio of MOF to the crosslinked polymer network in the MOF-PMAi-Br composite was approximately 50:50, the presence of the bromosuccinimide groups was apparent and the active bromine content was 1.8-1.9 mequiv/g. During TGA, MOF-PMAi-Br and PMAi-Br materials lost 20-35% of their initial mass, attributable to bromine, in the temperature ranges 200−360 °C. Degradation of the MOF organic linkers and PMAi network occurred at temperatures above 400°C, demonstrating high thermal stability of these organic components. XRD patterns (Fig.S9) showed that the materials possessed the crystalline MIL-101 topology, with or without the amorphous polymer, although the intensities of the MIL-101 peak positions in the 2-8 degree range were diminished in the

MOF-PMAi composite relative to those in the parent MIL-101(Cr) due to the presence of the X-ray absorbing polymer in the path of the beam. Brominated MOF-PMAi-Br showed a distinct MIL-101 XRD pattern, matching well the patterns of the MIL-101(Cr) computed using lattice parameters obtained from the Cambridge Structural Database.

**Catalysis of fructose dehydration**

To elucidate the utility of the stable, porous and functional composite materials developed in this work, we focused on the heterogeneous catalysis of the conversion of a bio-sourced substrate, fructose, into 5-hydroxymethylfurfural (HMF), one of the most important platform molecules for, e.g., liquid biofuel and polyester production, (Fig.S10). The conversion was studied in dimethylsulfoxide (DMSO), a common polar organic solvent for HMF synthesis. At a moderate temperature of 100$^{o}$C, the conversion of fructose to HMF was essentially complete after 1 h, as demonstrated by the disappearance of the α-anomeric proton signals of fructose in the 4.3-5.8 ppm range and appearance of signals at 6.59 (d, J=3.6 Hz, 1 H), 7.47 (d, J=3.6 Hz, 1H), and 9.54 (s, 1 H) characteristic of HMF (Fig.S11). Production of HMF was further confirmed by the $^{13}$C NMR spectra (Fig.S12), with the carbon signals at 56.4, 110.1, 124.8, 152.2, 162.6, and 178.3 ppm. After 1 h at 100$^{o}$C, the HMF fraction gradually declined, indicating conversion of HMF into other products. It is known that HMF is a transient product and can be decomposed to levulinic acid, polymerized to humic acids and converted to dialdehyde in the presence of oxidative species.[30] Since we were interested in quantifying the fructose-to-HMF conversion, we focused on the initial dehydration, and thus conducted the majority of measurements within the first hour of the reaction. The quantification was conducted by HPLC. Kinetics of D-fructose dehydration in DMSO at 100$^{o}$C and in the presence of MOF MIL-101(Cr), crosslinked and

brominated polymer network (PMAi-Br), and the composite hybrid network (MOF-PMAi-Br), are shown in Fig. 3.

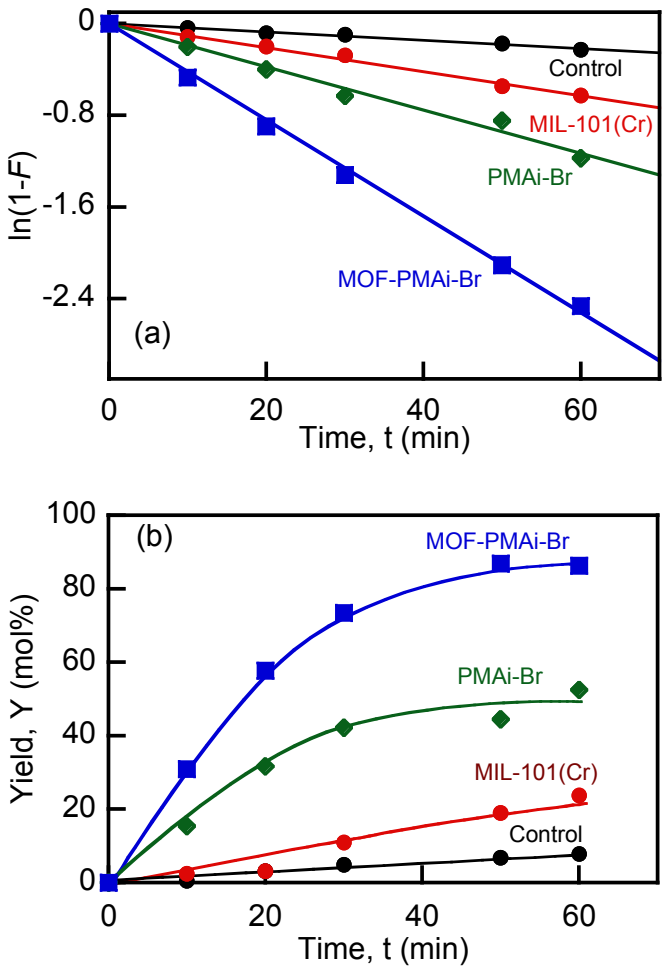


**Fig. 3.** Kinetics of D-fructose conversion (a) and HMF percent yield (b) at 100°C. Initial conditions: DMSO, 5 mL; D-fructose concentration ($C_{fo}$), 0.555 M; catalyst loading, 50 mg/mL. Control: no catalysts added. Liquid samples were withdrawn every 10 min and fructose concentration ($C_{ft}$) was measured by HPLC (RI detector) at each datum point, whereas HMF concentration ($C_{HMF}$) was measured by UV detection. Fructose conversion was defined as $F = 1 - C_{ft} / C_{f0}$.

Under the selected conditions, the initial kinetics of D-fructose conversion ($F$) to 5-hydroxymethylfurfural (HMF) could be described as pseudo-first order, with the assumptions (verified by NMR) that HMF was initially the main product and that the conversion of HMF itself to other products was a slow process. [24,26] Products other than HMF such as levulinic and formic acids could be also observed, but they were in the minority within a 1-hr reaction, not exceeding 5-10% of the main product, HMF. Under the pseudo-first order approximation, the fructose ($C_f$) and HMF ($C_{\mathrm{HMF}}$) concentrations in the reaction medium are related by an observed rate constant ($k_{\mathrm{obs}}$) as follows:

$$\frac{dC_f}{dt} = -\frac{dC_{\mathrm{HMF}}}{dt} = -k_{obs}C_f; \quad \text{i.e.,} \quad \ln(1-F) = -k_{obs}t$$

where $F = \Delta C_f / C_{f0}$ is the conversion degree; $\Delta C_f$ and $C_{f0}$ are the change in the fructose concentration and the initial fructose concentration, respectively.

As shown in Fig. 3a, the conversion kinetics were described well by the pseudo-first order model, with excellent linear fits in the coordinates of eqn (1) ($R^2 > 0.98$ in all cases). The reaction was also pseudo-first order with respect to the initial MOF-PMAi-Br (catalyst) (Fig.S13), so the final rate expression is

$$\frac{dC_f}{dt} = -k''C_{cat}C_f$$

where $k''$ is a second order rate constant, and $C_{cat}$ is the catalyst concentration. We obtain an estimated value of $k''$ to be 9.2 x$10^{-4}$ $\mathrm{min}^{-1}$ $(\mathrm{mg/mL})^{-1}$, which compares favorably with 5.6 x $10^{-4}$ $\mathrm{min}^{-1}$ $(\mathrm{mg/mL})^{-1}$ reported recently for the fructose conversion at 100°C in DMSO using MOF MIL-101(Cr) modified with sulfonic groups as a catalyst (MIL-101(Cr)-$SO_3H$).[32] The activation

energy ($E_a$) for the fructose transformation over the 80-140°C range was 53 kJ/mol (Fig.S14). Analogously, the D-fructose conversion reactions have been found to be of the first order with respect to the fructose concentration in DMSO without catalysts [21] and with MOF MIL-101(Cr) modified with sulfonic groups as catalysts (MIL-101(Cr)-$SO_3H$).[32]

Comparison of the MOF-PMAi-Br material with other heterogeneous catalysts including solid acids is favorable. In our case, the values of $k_{obs}$ (2.97 $h^{-1}$) and activation energy (53 kJ/mol) show a higher catalytic activity of MOF-PMAi-Br in the fructose conversion in DMSO than the acidic MIL-101(Cr)-$SO_3H$ (15% sulfonic groups) catalyst ($k_{obs}$ and $E_a$, 2.01 and 55 kJ/mol, respectively). An additional advantage of the MOF-PMAi-Br material over solid acid catalysts such as MIL-101(Cr)-$SO_3H$ is its higher versatility due to the high content of halamine (>N-Br) groups known for their mild oxidative and bromination action in a variety of reactions.[20]

The HMF concentration increased gradually and plateaued at a yield of around 86-87% at high degrees of the fructose conversion ($F$ around 0.95-0.97) with MOF-PMAi-Br as a catalyst, but did not decay over the course of the 1-h reaction, thus supporting the hypothesis of the slow conversion of the evolved HMF (Fig. 3b).

It is interesting to observe that some HMF formation was detected in DMSO without any acid or solid catalyst added, in accordance with the notion that DMSO itself can facilitate, albeit less efficiently, the fructose dehydration at elevated temperatures.[21,33-35] The presence of MIL-101(Cr) at 50 mg/mL level increased both the rate of the fructose conversion (reaction half-life 1.1 h) and HMF production, with the HMF yield reaching 24% after 1 h at 100°C. MOF MIL-101(Cr) is known to possess Lewis acid functionality due to the presence of unsaturated chromium sites (CUS) formed upon removal of water or solvent molecules from the chromium

clusters of the MOF. [35,36] This material has been tested previously (upon activation to free up CUS) for its ability to catalyze carbohydrate dehydration. [32,37] In the presence of activated MIL-101(Cr), at a temperature of 80 °C, the HMF yields were negligible [32] and at 120°C the HMF yield was observed to be low at 24%. [23] We surmise that the Cr(III) centers in MIL-101(Cr) are not sufficiently active in the dehydration of carbohydrates. MOF modification by incorporation of strongly acidic polyoxometalate molecules into its pores or by attachment of sulfonic acid groups through the terephthalic acid (MOF linker) sulfonation affords significant enhancement of the MOF performance as a heterogeneous catalyst in the carbohydrate dehydration. [32,37,38]

In the present work, we employed poly(N-bromomaleimide-*co*-divinylbenzene) (PMAi-Br) as a source of active bromine capable of monosaccharide oxidation. PMAi-Br is a polymeric, water- and solvent-insoluble analogue of N-bromosuccinimide (NBS). The latter has been proven to mediate oxidation and dehydration of D-fructose and some other monosaccharides in aqueous acidic and polar organic solvent media.[39-44] NBS is a good source of electrophilic bromine in polar solvents, which is why it has numerous applications in organic chemistry, and NBS-DMSO in particular is a facile oxidation catalyst generating "activated DMSO" and nucleophilic bromide species (Fig. S15).[45-47] As we have demonstrated,[20] PMAi-Br is a versatile oxidant in reactions with phosphorothioates, thioethers, and hydrazines due to the polymer's active bromine. In the current work, the presence of PMAi-Br accelerated the D-fructose conversion approximately 5-fold (reaction half-life, 37 min) compared to the reaction in DMSO only (Fig.3a), and significantly enhanced the HMF yield, with Y reaching 50% after 1 h (Fig.3b). However, when PMAi-Br was incorporated into the composite network with MIL-101(Cr), the resulting material exceeded the activity of PMAi-Br significantly, despite the 2-fold lower effective bromine content, and exhibited synergism between the MOF and the brominated

polymer as a promoter of the D-fructose conversion, with the reaction half-life at 100°C less than 14 min and HMF yield reaching 85-87% after 1 h. The yield of HMF and the fructose conversion rate with MOF-PMAi-Br compare favorably with most previously reported catalysts. For example, in fructose conversion catalyzed in DMSO by N-methyl-2-pyrrolidonium methyl sulfonate in DMSO or by $SnCl_4$–tetrabutyl ammonium bromide, also in DMSO at 90-100°C, the yield of HMF after 2-h reaction was reported to be 69.1-69.4%.[48,49] An HMF yield of 83 % was achieved in an ionic liquid such as 1-ethyl-3-methylimidazolium chloride, with $CrCl_2$ as catalyst at a temperature of 80 °C for a reaction time of 3 h.[50] Analogously, an HMF yield of 96% was observed at 100 °C after 6 h reaction time in 1-butyl-3-methyl imidazolium chloride, also using $CrCl_2$ as catalyst. [51] A disadvantage of such systems, however, is that the product cannot be separated from the ionic liquid catalysts without significant input of energy; such a disadvantage is not shared with solid, heterogeneous catalysts, which can be readily separated from the reaction mixture and recycled in an environmentally friendly process for saccharide conversion and biofuel production.[52] Acids are well-known to induce saccharide dehydration when added to a porous solid to form a heterogeneous catalyst, the activity of which is a function of the acidic group content.

Good accessibility of the reactive sites by the reactants is crucial for the solid catalyst efficiency.[52] The MOF-PMAi-Br material possesses a surface area that is at least two orders of magnitude higher than that of the PMAi-Br polymer network, and that explains the higher catalytic activity of the composite (Fig.4). Mechanistically, the synergistic action of the composite MOF-PMAi-Br material can be traced to the MIL-101(Cr) structure and the ability of the $Cr^{3+}$ ions to coordinate with the carboxyls of the 1,4-benzene dicarboxylate, solvents and water during the MOF synthesis and subsequent exchange of bromide formed at the PMAi-Br

chains in the immediate proximity to the $Cr^{3+}$ clusters. The MIL-101(Cr) framework consists of terephthalate linkers and $Cr_3O$-carboxylate trimers with octahedrally coordinated metal ions binding terminal water or other solvent molecules.[27,53] The terminal water molecules can be removed readily by thermal treatment under vacuum, resulting in the appearance of CUS. Our synthesis procedure, which involves copolymerization of maleimide (Mal) and divinylbenzene within the porous structure of the activated MIL-101(Cr) followed by the workup and bromination of the resultant hybrid material with $Br_2$, can promote formation of the bromide anions from the N-bromomaleimide units of the PMAi-Br, in a reaction where resultant succinimide units are complexed with the coordinated $Cr^{3+}$ cations (Fig.4)

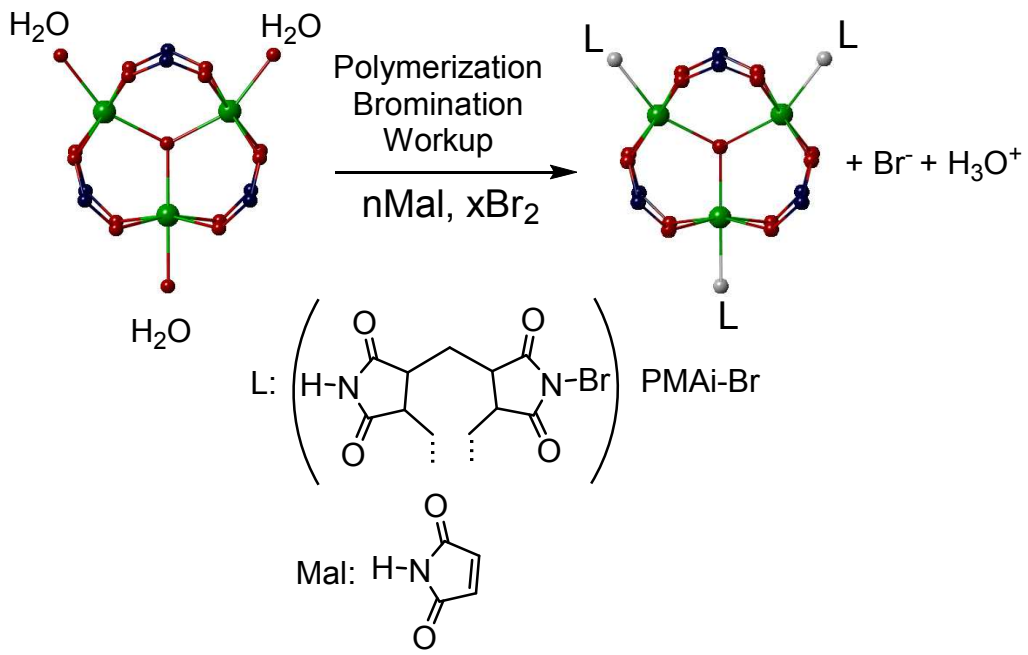


Fig.4. Schematic representation of the MIL-101(Cr) trimeric building block sharing an oxygen center and chelated by six carboxylates, with CUS sites coordinated with water molecules. Upon polymerization of N-maleimide (Mal), workup of the resulting hybrid polymer/MOF network, and subsequent bromination, the CUS sites become coordinated with Mal units of the PMAi-Br network as ligands (L), while bromide evolves. Chromium, oxygen, and carbon atoms are in green, red, and blue, respectively. Formation of mixed $Cr^{3+}$-carboxylate-succinimide complexes

is known, [54-56] and substitution of coordinated water or solvent ligands in MIL-101(Cr) for other terminal ligands such as pyridines, amines, and different solvent molecules is well-documented.

The notion of MOF and brominated polymer coordination, coupled with the presence of the bromide and bromine in the hybrid MOF-PMAi-Br network, can explain the facilitation of the fructose dehydration by the hybrid material via nucleophilic attack by the $Br^-$ ion on the fructose (Fig. 6).

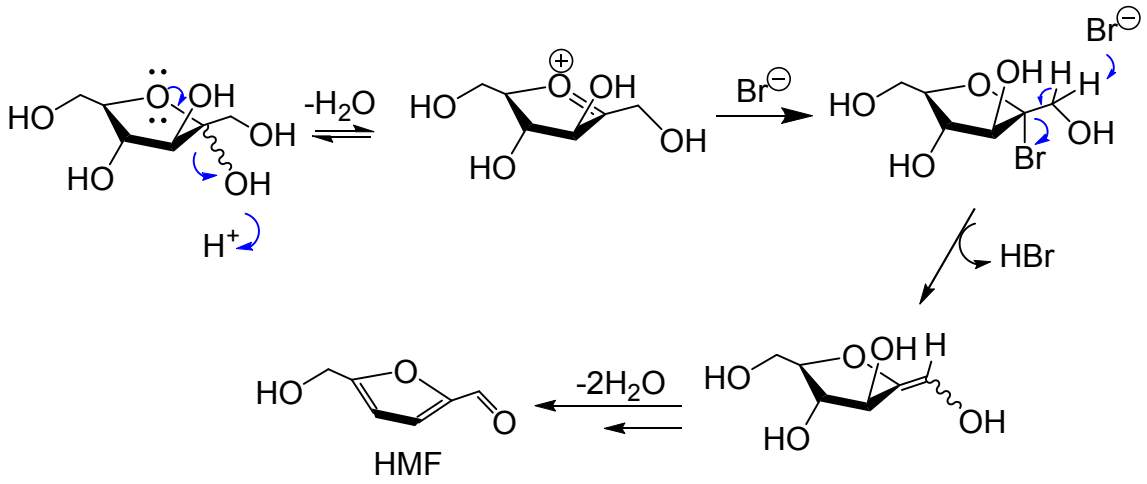


Fig.5. Putative mechanism of the fructose dehydration via nucleophilic attack by bromide.[57,58]

The formation of the fructofuranosyl oxocarbenium ion at the beginning of the fructose dehydration (Fig.5) with the spontaneous release of a proton at the C-1 position to form the enol furan intermediate is most often implied because it is energetically favored and more stable.[34,58-62] The oxocarbenium ion is attacked by a bromide ion with the formation of relatively stable 2-deoxy-2-bromo intermediate that is less prone to revert back to fructose.[58] The intermediate then releases HBr to form the enol that loses two water molecules to yield 5-HMF.

The role of chromium salts and complexes in the monosaccharide conversion catalysis is often emphasized in the case of hexoses such as glucose, where the chromium compound enables

conversion of the glucose to HMF by initially catalyzing the isomerization of glucose into fructose, followed by dehydration.[58] Chromium present in solution likely forms multicoordinate complexes with the hydroxyl groups of glucose, catalyzing its isomerization. In our experiments with MOF-PMAi-Br, the yield of HMF from glucose in DMSO at 100$^{o}$C was only 7 and 16% after 2 and 6-h reaction, respectively (initial catalyst and glucose concentrations, 50 mg/mL and 0.55M, respectively). The poor HMF yield from glucose can be explained by the absence of chromium in solution, supporting the conclusion that chromium did not leach from the composite into the solution, and by an overall low availability for the hexose of the CUS complexed with the polymer. On the other hand, abundantly available halamine groups do not specifically catalyze glucose isomerization.

**Catalyst reuse**

The implied participation of the bromine and bromide ions formed within the MOF-PMAi-Br material in fructose dehydration suggests that some of the bromine initially present in the >N-Br group of the N-bromomaleimide units of the PMAi-Br component of the composite material can be lost when the formed bromide is released into the reaction medium. We conducted "hot filtration" tests to investigate whether catalyst components that might leach into DMSO from the MOF-PMAi-Br composite would enable fructose conversion into HMF when the solid catalyst is removed (Fig. 6).

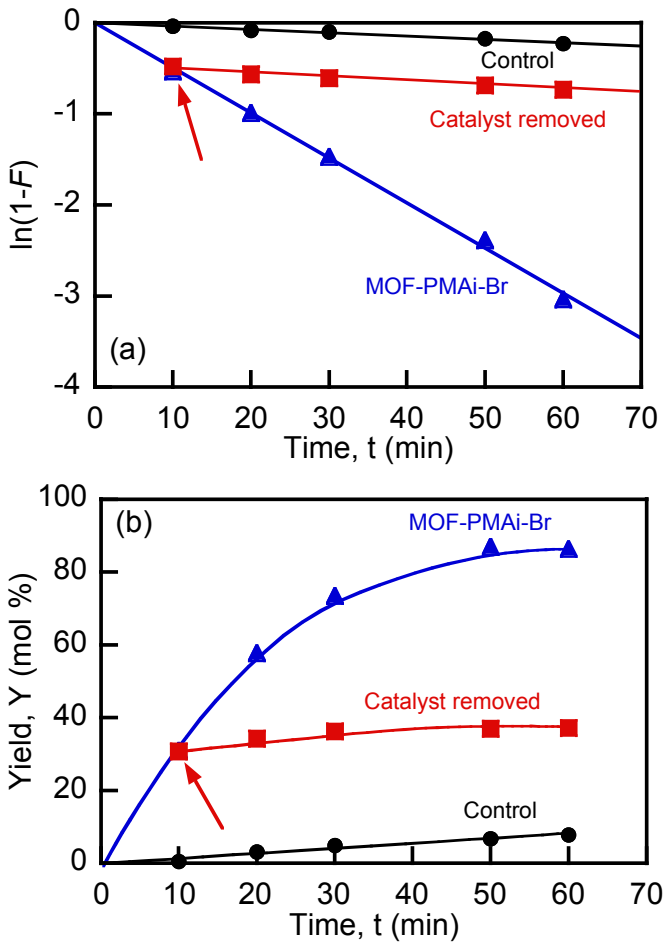


**Fig. 6**. Effect of catalyst removal on kinetics of D-fructose conversion (a) and HMF yield (b) in DMSO at 100°C. Initial conditions: DMSO, 5 mL; D-fructose concentration ($C_{fo}$), 0.555 M; catalyst MOF-PMAi-Br loading, 50 mg/mL. Control: no catalyst added. The reaction was allowed to commence with the catalyst; at t=10 min a sample was withdrawn for fructose measurement; at t=12 min, the catalyst was removed by centrifugation at 12,000 *g* for 1 min. The supernatant separated from the catalyst was subjected to a further kinetic study at 100°C. Catalyst removal event is shown by arrows.

Upon catalyst removal, the fructose conversion rate slowed down to become approximately equal to that observed in DMSO in the control experiment without any catalyst. Analogously, the HMF yield plateaued, increasing only 3-5% after the catalyst was removed, consistent with

fructose dehydration conversion rates in DMSO only. Elemental analysis yielded bromine and chromium concentrations in DMSO after catalyst removal to be 72 and < 2 mg/L (<detection limit), respectively, showing that approximately 1% of the bromine and only insignificantly small amounts of chromium initially present in the catalyst leached into the reaction medium. The leached bromine failed to facilitate the fructose conversion rate beyond that observed in DMSO without any bromine. These experiments demonstrate that, from a practical standpoint, the MOF-PMAi-Br material acts as a heterogeneous catalyst in the fructose dehydration process.

We were interested in exploring the recyclability of MOF-PMAi-Br (Fig.7). In each cycle, the material was removed from the reaction medium after 1-h reaction at 100°C, washed and worked up as described in Experimental.

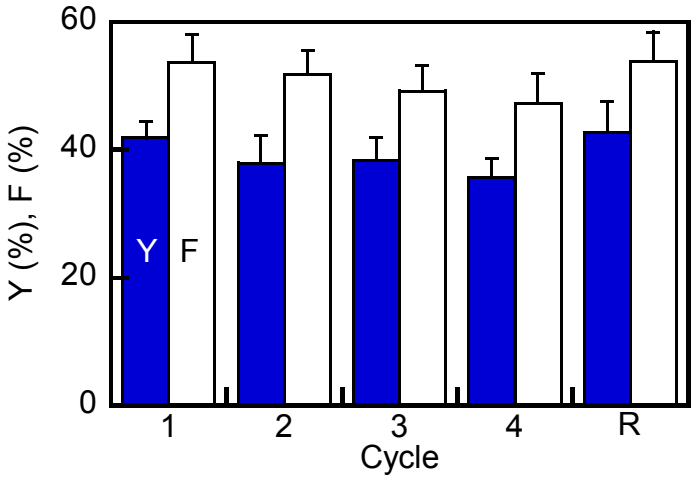


Fig. 7. HMF yield (Y, filled columns) and fructose conversion (F, open columns) after 1-h reaction catalyzed by MOF-PMAi-Br at 100°C in DMSO in five consecutive cycles. Cycle R refers to the catalyst regeneration by bromination after the 4-th cycle. Initial conditions: DMSO, 5 mL; D-fructose concentration ($C_{f0}$), 0.555 M; catalyst MOF-PMAi-Br loading, 25 mg/mL.

Elemental analysis of the reaction medium in the recycling experiments yielded effective bromine concentrations of 56-98 mg/L, which indicated that 1.3-2.8% bromine initially present

on MOF-PMAi-Br was released into the reaction medium in each of the consecutive cycles. Powder XRD of the catalyst recovered after the recycling (Fig. S16) demonstrated that the MOF crystal structure remained intact, although there was some reduction in the peak intensity, which probably indicated the presence of amorphous organic matter.

By the fourth cycle, the yield of HMF and fructose conversion degree had declined by approximately 6% compared to the first cycle. The accessibility of the bromine in the catalyst might have been impacted by the sorption of the polymeric reaction products (humines) within the catalyst pores.[25,63-64] After four cycles, only 3-4% of the catalyst mass was lost. The selectivity for HMF production was high, ranging from 73 to 78%, and did not decline with catalyst reuse. Notably, regeneration by bromination of the catalyst recovered after the fourth cycle completely restored the MOF-PMAi-Br activity (Fig. 7). A small amount of the MOF-PMAi-Br material (25 mg containing 45 umol of bromine) converted over 1.9 g (11 mmol) of D-fructose in four cycles, indicating a remarkable performance figure of merit for that catalyst.

**Concluding remarks**

A facile and straightforward method to fabricate novel composite organic and coordinate polymeric networks with high surface area, mesoporous structure, and high content of functional groups has been introduced. In this approach, vinyl monomers and crosslinkers impregnated within MOF pores undergo free-radical polymerization to form a cross-linked polymer network threading through the MOF porous structure; these polymers can be functionalized readily to imbue them with catalytic properties. While in this work the functional groups are exemplified by the N-bromomaleimide units obtained via bromination, analogous post-synthetic functionalization of the composite by other groups is readily achievable. Stability of the

composite material in solvents was enabled both by the chemical and structural stability of the parent MOF and by the design of the cross-linked polymeric network. We demonstrated that the composite material is an effective, recyclable, heterogeneous catalyst for fructose dehydration into 5-hydroxymethylfurfural (HMF), which is a versatile intermediate in the production of high value chemicals such as alternative fuels, diesel fuel additives, industrial solvents and bio-derived polymers.

**Supporting Information**

Detailed procedures of MOF synthesis, NMR experiments, detailed description of hot filtration experiments, SEM and TEM images, BET adsorption isotherms, TGA curves, FTIR, XRD, XPS, $^{1}$H and $^{13}$C NMR spectra, dependences of the observed rate constant of D-fructose conversion on the initial catalyst loading and temperature. This material is available free of charge via the Internet at http://pubs.acs.org.

The authors declare no competing financial interest.

**References**


1. Chae, H.K.; Siberio-Pérez, D.Y.; Kim, J.; Go, Y.; Eddaoudi, M.; Matzger, A.J.; O'Keeffe, M.; Yaghi, O.M. *Nature*, **2004**, *427*(6974), 523-527.
2. Morozan, A.; Jaouen, F. *Energy Environ. Sci*., **2012**, *5*, 9269-9290.
3. Furukawa, H.; Cordova, K.E.; O'Keeffe, M.; Yaghi, O.M. *Science*. **2013**, *341*(6149), 1230444.
4. Horike, S.; Umeyama, D.; Kitagawa. S. *Acc. Chem. Res*. **2013**, *46*, 2376-2384.
5. Evans, J.D.; Sumby, C.J.; Doonan. C.J. *Chem. Soc. Rev*., **2014**, *43*, 5933-5951.
6. Sun, J.-K.; Xu, Q. *Energy Environ. Sci*., **2014**, *7*, 2071-2100.

7. Gándara, F.; Furukawa, H.; Lee, S.; Yaghi, O.M. *J. Am. Chem. Soc*. **2014**, *136*, 5271-5274.

8. Zhang, L.; Su, Z.; Jiang, F.; Yang, L.; Qian, J.; Zhou, Y.; Li W.; Hong, M. *Nanoscale*, **2014**, *6*, 6590-6602.

9. Holst, J. R.; Cooper, A. I. *Adv. Mater*., **2010**, *22*, 5212–5216.

10. Ben, T.; Ren, H.; Ma, S.; Cao, D.; Lan, J.; Jing, X.; Wang, W.; Xu, J.; Deng, F.; Simmons, J. M.; Qiu, S.; Zhu, G. *Angew.Chem*., **2009**, *121*, 9621–9624.

11. Comotti, A.; Bracco, S.; Mauri, M.; Mottadelli, S.; Ben, T.; Qiu, S.; Sozzani, P. *Angew.Chem.Int.Ed*.; **2012**, *51*, 10136–10140.

12. Podsiadlo, P.; Kaushik, A. K.; Arruda, E. M.; Waas, A. M.; Shim, B. S.; Xu, J.; Nandivada, H.; Pumplin, B. G.; Lahann, J.; Ramamoorthy, A.; Kotov, N. A. *Science*, **2007**, *318*, 80-83.

13. Uemura, T.; Horike, S.; Kitagawa, K.; Mizuno, M.; Endo, K.; Bracco, S.; Comotti, A.; Sozzani, P.; Nagaoka, M.; Kitagawa, S. *J. Am. Chem. Soc*. **2008**, *130*, 6781-6788.

14. Kageyama, K.; Tamazawa, J.; Aida, T. *Science,* **1999**, *285*, 2113-2115.

15. Uemura, T.; Yanai, N.; Kitagawa, S. *Chem. Soc. Rev*. **2009**, *38*, 1228-1236.

16. Distefano, G.; Suzuki, H.; Tsujimoto, M.; Isoda, S.; Bracco, S.; Comotti, A.; Sozzani, P.; Uemura, T.; Kitagawa, S. *Nature Chem*. **2013**, *5*, 335-341.

17. Gao, L.; Li, C.-Y. V.; Chan, K.-Y.; Chen, Z.-N. *J. Am. Chem. Soc*. **2014**, *136*, 7209−7212.

18. Juan-Alcañiz, J.; Ramos-Fernandez, E. V.; Lafont, U.; Gascon, J.; Kapteijn, F. *J. Catal.* **2010**, *269*, 229–241.

19. Bromberg, L.; Diao, Y.; Wu, H.; Speakman, S. A.; Hatton, T. A. *Chem. Mater*. **2012**, *24*, 1664−1675.

20. L. Bromberg, N. Pomerantz, H. Schreuder-Gibson, T. A. Hatton, *Ind.Eng.Chem.Res*., **2014**, DOI: 10.1021/ie501055g.

21. Amarasekara, A.S.; Williams L.D.; Ebede, C.C. *Carbohydrate Res*., **2008**, *343*, 3021-3024.

22. Kimura, H.; Nakahara, M.; Matubayasi, N. *J. Phys. Chem. A*, **2013**, *117*, 2102–2113.

23. Tian, G.; Tong, X.; Wang, Y.; Yan, Y.; Xue, S. *Res. Chem. Intermed*., **2013**, *39*, 3255-3263

24. Qi, X.; Watanabe, M.; Aida, T.M.; Smith, R.L. *Green Chem*., **2009**, *11*, 1327-1331.

25. Román-Leshkov, Y.; Chheda, J. N.; Dumesic, J. A. *Science*, **2006**, *312*, 1933-1937.

26. Lee, Y.-Y.; Wu, K. C.-W. *Phys. Chem. Chem. Phys*., **2012**, *14*, 13914-13917.

27. Maksimchuk, N.V.; Zalomaeva, O. V., Skobelev, I. Y.; Kovalenko, K. A.; Fedin, V. P.; Kholdeeva, O. A., *Proc. R. Soc. A*., **2012**, *468*, 2017-2034.

28. Valvekens, P.; Vermoortele, F.; De Vos, D. *Catal. Sci.Technol*., **2013**; *3*, 1435-1445.

29. Hwang, Y.K.; Fèrey, G.; Lee, U.-H.; Chang, J.-S. Chapter 8, In: *Liquid Phase Oxidation via Heterogeneous Catalysis: Organic Synthesis and Industrial Applications*, Ed. by Clerici, M. G.; Kholdeeva, O. A. John Wiley & Sons, **2013**, 371-405.

30. Gascon, J.; Corma, A.; Kapteijn, F.; Llabrés i Xamena, F.X. *ACS Catal*., **2014**, *4*, 361–378.

31. Lewkowski, J. *Arkivos*, **2001**(***i***), 17-54.

32. Chen, J.; Li, K.; Chen, L.; Liu, R.; Huang, X.; Ye, D. *Green Chem*., **2014**, *16*, 2490-2499.

33. Musau, R.M.; Munavu, R.M. *Biomass* **1987**, *13*, 67-74.

34. Akien, G. R.; Qi, L.; Horváth, I. T. *Chem. Commun*., **2012**, *48*, 5850-5852.

35. Vimont, A.; Goupil, J.M.; Lavalley, J.C.; Daturi, M.; Surblé, S.; Serre, C.; Millange, F.; Férey, G.; Audebrand N. *J. Am. Chem. Soc*. **2006**, *128*, 3218-3227.

36. Wang, S.; Bromberg, L.; Schreuder-Gibson, H.; Hatton, T.A. *ACS Appl. Mater. Interfaces.* **2013**, *5*, 1269-1278.

37. Zhang, Y.; Degirmenci, V.; Li, C.; Hensen, E.J.M. *ChemSusChem*, **2011**, *4*, 59–64.

38. Akiyama, G.; Matsuda, R; Sato, H.; Takata, M.; Kitagawa, S.; *Adv. Mater*. **2011**, *23*, 3294-3297.

39. Singh, A. K.; Srivastava, R.; Srivastava, S.; Srivastava, J.; Rahmani, S.; Singh, B. *J. Mol. Catal. A: Chem*. **2009**, *310*, 64-74.

40. Singh, A. K.; Rahmani, S.; Singh, V.; Gupta, V.; Singh, B. *Oxid.Commun*. **2000**, *23*, 55-61.

41. Singh, A. K.; Rahmani, S.; Singh, V. K.; Gupta, V.; Kesarwani, D.; Singh, B. *Ind. J. Chem.* **2001**, *40A*, 519-523.

42. Tian, G.; Tong, X.; Wang, Y.; Yan, Y.; Xue, S. *Res. Chem. Intermed*., **2013**, *39*, 3255-3263.

43. Singh, A.K.; Singh, P.; Srivastava, J.; Jaya, Rahmani, S.; Singh, S.K. J.Energy Chem. Eng., **2014**, *2*, 8-22.

44. Wolfe, S.; Pilgrim, W.R.; Garrard, T.F.; Chamberlain, P. *Can J.Chem*., **1971**, *49*, 1099-1105.

45. Uzagare, M.C.; Padiya, K.J.; Salunkhea, M.M.; Sanghvi, Y.S. *Bioorg.Med. Chem. Lett*. **2003**, *13*, 3537–3540.

46. Tojo, G.; Fernandez, M.I. In: *Oxidation of Alcohols to Aldehydes and Ketones. A Guide to Current Common Practice*, Springer, 2006, Chapter 2, pp. 97-179.

47. Tong, X.; Li, Y. *ChemSusChem*, **2010**, *3*, 350–355.

48. Tian, G.; Tong, X.; Cheng, Y.; Xue, S.; *Carbohydrate Res*., **2013**, *370*, 33–37.

49. Zhao, H.; Holladay, J.E.; Brown, H.; Zhang, Z.C. *Science*, **2007**, *316*, 1597-1600.

50. Yong, G.; Zhang, Y.; Ying, J.Y. *Angew. Chem*., **2008**, *120*, 9485–9488.

51. Guo, F.; Fang, Z.; Xu, C.C.; Smith R.L.; *Progr. Energy Combustion Sci*. **2012**, *38*, 672-690.

52. Asghari, F. S.; Yoshida, H. *Ind. Eng. Chem. Res*., **2006**, *45*, 2163–2173.

53. Férey, G.; Mellot-Draznieks, C.; Serre, C.; Millange, F.; Dutour J.; Surblé S.; Margiolaki, I. *Science*, **2005**, *309*, 2040-2042.

54. Islam, M. S.; Uddin, M.M. Synthesis and Reactivity in Inorganic and Metal-Organic Chemistry, **1992**, *22*, 1303-1315.

55. da Silva, A.G.M.; Rodrigues, T.S.; Gurgel, L.V.A.; Assis, P.A.; Gil, L.F.; Robles-Dutenhefner, P.A. *Industrial Crops and Products* **2013**, *50*, 288– 296.

56. Llabrés i Xamena, F.X.; Luz, I.; Cirujano, F.C. In: *Metal Organic Frameworks as Heterogeneous Catalysts*, Ed. by Llabrés i Xamena, F.X.; Gascon, J. RSC Catalysis Series No. 12; RSC Publishing, Cambridge, UK, 2013 Chapter 7, pp.237-267.

57. Binder, J.B.; Raines, R.T. *J. Am. Chem. Soc*. **2009**, *131*, 1979–1985.

58. Ståhlberg, T.; Sørensen, M.G.; Riisager, A. *Green Chem*., **2010**, *12*, 321–325.

59. Antal, M.J.; Mok, W. S. L.; Richards, G. N. *Carbohydrate Res*. **1990**, *199*, 91-109.

60. Bing, L.; Zhang, Z.; Deng, K. *Ind. Eng. Chem. Res*., **2012**, *51*, 15331–15336.

61. Mittal, N.; Nisola, G.M.; Chung, W.-J. *Tetrahedron Let*.; **2012**, *53*, 3149-3155.

62. Chheda, J. N.; Roman-Leshkov, Y.; Dumesic, J. A. *Green Chem*., **2007**, *9*, 342–350.

63. Torres, A. I.; Daoutidis, P.; Tsapatsis M., *Energy Environ. Sci*., **2010**, *3*, 1560–1572.

64. Zhang, Y.; Pan, J.; Gan, M.; Ou, H.; Yan, Y.; Shib, W.; Yu, L., *RSC Adv*., **2014**, *4*, 11664–11672.

Table of Contents